

HEPHY-PUB 784/04
hep-ph/0401092

Complete one-loop corrections to $e^+e^- \rightarrow \tilde{f}_i \tilde{\bar{f}}_j$

K. Kovařík^{1,2}, C. Weber¹, H. Eberl¹, W. Majerotto¹

¹*Institut für Hochenergiephysik der Österreichischen Akademie der Wissenschaften,
A-1050 Vienna, Austria*

²*Department of Theoretical Physics FMFI UK, Comenius University,
SK-84248 Bratislava, Slovakia*

Abstract

We have calculated the complete one-loop corrections to the sfermion pair production process $e^+e^- \rightarrow \tilde{f}_i \tilde{\bar{f}}_j$ ($f = t, b, \tau, \nu_\tau$) in the Minimal Supersymmetric Standard Model. Our results also include the previously calculated SUSY-QCD corrections. We present the details of the renormalization scheme used. It is found that the weak corrections are of the same magnitude as the SUSY-QCD corrections at higher energies ($\sqrt{s} \sim 1\text{TeV}$). At these energies the main part of the weak corrections stems from the box contribution. This is best seen in sneutrino production.

1 Introduction

If supersymmetry (SUSY) is realized in Nature there should be two scalar particles (sfermions) \tilde{f}_L , \tilde{f}_R corresponding to the two chirality states of each fermion f . The sfermions of the third generation play a special role as \tilde{f}_L and \tilde{f}_R may strongly mix (proportionally to the fermion mass), forming the two mass eigenstates \tilde{f}_1 and \tilde{f}_2 (with $f = t, b, \tau$) . As a consequence one eigenstate (\tilde{f}_1) can have a much lower mass than the other one.

Sfermion pair production in e^+e^- collisions, $e^+e^- \rightarrow \tilde{f}_i \bar{\tilde{f}}_j$, ($i, j = 1, 2$), has been studied extensively phenomenologically [1]. The strong interest in sfermion production is mainly due to the fact that it gives access to one of the fundamental SUSY breaking parameters A_f , the trilinear coupling parameter. It is clear that in $e^+e^- \rightarrow \tilde{t}_i \bar{\tilde{t}}_j$ and $\tilde{b}_i \bar{\tilde{b}}_j$ gluon radiation and gluon exchange play an important role [2, 3]. The SUSY-QCD corrections to these processes due to gluino and squark exchange were calculated in [4, 5] and found to become effective at $\sqrt{s} > 500$ GeV. Yukawa corrections [6] were shown to be non negligible either. Very recently, while we were already working on the calculation of the full one-loop corrections to sfermion pair production within the Minimal Supersymmetric Standard Model (MSSM), such a calculation was presented in [7]. In this context, it is worthwhile to mention that the complete one-loop corrections to selectron and smuon pair production from threshold to high energies were calculated in [8].

For the calculation of higher order corrections, renormalization of the MSSM with an appropriate fixing of the SUSY parameters is necessary. Essentially, two methods were proposed in the on-shell scheme, one in [9, 10] and the other one in [11, 12] for a review see [13]. Of course, both should lead to the same results for observables as masses, cross-sections, widths , etc.. The schemes differ in the fixing of the counterterms of some of the SUSY parameters as M_1, M_2, μ , etc. Therefore the meaning of these parameters is different at loop level. However, at one-loop, in sfermion pair production this difference only matters in selectron pair production, $e^+e^- \rightarrow \tilde{e}_i \bar{\tilde{e}}_j$, and sneutrino pair production, $e^+e^- \rightarrow \tilde{\nu}_e \bar{\tilde{\nu}}_e$, due to the neutralino or chargino exchange being already present at tree level. In our case, we have a different fixing of the fine structure constant α taking $\alpha(m_Z)$ as input, in contrast to [7] where the Thomson limit is used according to [14].

In this paper, we also present a full one-loop calculation within the MSSM for $e^+e^- \rightarrow \tilde{f}_i \bar{\tilde{f}}_j$, $f = t, b, \tau, \nu_\tau$. We compare our results with those obtained in [7]. Due to the complexity of such a calculation, an independent computation seems appropriate. We have calculated all graphs analytically and have written our own computer program for the numerical evaluation. Checks have been performed using the computational package [15, 16]. In addition to the comparison with [7], we studied different physical scenarios in our numerical analysis. We also include a study of the tau-sneutrino production which was not presented elsewhere.

2 Tree-level

The sfermion mixing is described by the sfermion mass matrix in the left-right basis $(\tilde{f}_L, \tilde{f}_R)$, and in the mass basis $(\tilde{f}_1, \tilde{f}_2)$, $f = t, b$ or τ [17, 18],

$$\mathcal{M}_{\tilde{f}}^2 = \begin{pmatrix} m_{\tilde{f}_L}^2 & a_f m_f \\ a_f m_f & m_{\tilde{f}_R}^2 \end{pmatrix} = (R^{\tilde{f}})^\dagger \begin{pmatrix} m_{\tilde{f}_1}^2 & 0 \\ 0 & m_{\tilde{f}_2}^2 \end{pmatrix} R^{\tilde{f}}, \quad (1)$$

where $R_{i\alpha}^{\tilde{f}}$ is a 2×2 rotation matrix with rotation angle $\theta_{\tilde{f}}$, which relates the mass eigenstates \tilde{f}_i , $i = 1, 2$, ($m_{\tilde{f}_1} < m_{\tilde{f}_2}$) to the weak eigenstates \tilde{f}_α , $\alpha = L, R$, by $\tilde{f}_i = R_{i\alpha}^{\tilde{f}} \tilde{f}_\alpha$ and

$$m_{\tilde{f}_L}^2 = M_{\{\tilde{Q}, \tilde{L}\}}^2 + (I_f^{3L} - e_f \sin^2 \theta_W) \cos 2\beta m_Z^2 + m_f^2, \quad (2)$$

$$m_{\tilde{f}_R}^2 = M_{\{\tilde{U}, \tilde{D}, \tilde{E}\}}^2 + e_f \sin^2 \theta_W \cos 2\beta m_Z^2 + m_f^2, \quad (3)$$

$$a_f = A_f - \mu (\tan \beta)^{-2I_f^{3L}}. \quad (4)$$

$M_{\tilde{Q}}$, $M_{\tilde{L}}$, $M_{\tilde{U}}$, $M_{\tilde{D}}$ and $M_{\tilde{E}}$ are soft SUSY breaking masses, A_f is the trilinear scalar coupling parameter, μ the higgsino mass parameter, $\tan \beta = \frac{v_2}{v_1}$ is the ratio of the vacuum expectation values of the two neutral Higgs doublet states, I_f^{3L} denotes the third component of the weak isospin of the fermion f , e_f the electric charge in terms of the elementary charge e , and θ_W is the Weinberg angle.

The mass eigenvalues and the mixing angle in terms of the primary parameters are

$$m_{\tilde{f}_{1,2}}^2 = \frac{1}{2} (m_{\tilde{f}_L}^2 + m_{\tilde{f}_R}^2 \mp \sqrt{(m_{\tilde{f}_L}^2 - m_{\tilde{f}_R}^2)^2 + 4a_f^2 m_f^2}) \quad (5)$$

$$\cos \theta_{\tilde{f}} = \frac{-a_f m_f}{\sqrt{(m_{\tilde{f}_L}^2 - m_{\tilde{f}_R}^2)^2 + a_f^2 m_f^2}} \quad (0 \leq \theta_{\tilde{f}} < \pi), \quad (6)$$

and the trilinear breaking parameter A_f can be written as

$$m_f A_f = \frac{1}{2} (m_{\tilde{f}_1}^2 - m_{\tilde{f}_2}^2) \sin 2\theta_{\tilde{f}} + m_f \mu (\tan \beta)^{-2I_f^{3L}}. \quad (7)$$

The mass of the sneutrino ν_τ is given by $m_{\nu_\tau}^2 = M_L^2 + \frac{1}{2} m_Z^2 \cos 2\beta$.

The tree-level cross-section of $e^+ e^- \rightarrow \tilde{f}_i \tilde{f}_j$ is given by

$$\sigma^{\text{tree}}(e^+ e^- \rightarrow \tilde{f}_i \tilde{f}_j) = \frac{N_C}{3} \frac{\kappa^3(s, m_{\tilde{f}_i}^2, m_{\tilde{f}_j}^2)}{16 \pi s^2} (T_{\gamma\gamma} + T_{\gamma Z} + T_{ZZ}), \quad (8)$$

where

$$T_{\gamma\gamma} = \frac{e^4 e_f^2 (\delta_{ij})^2}{s^2} \frac{1}{2} (K_L^2 + K_R^2), \quad (9)$$

$$T_{\gamma Z} = -\frac{g_Z^2 e^2 e_f a_{ij}^{\tilde{f}} \delta_{ij}}{4s(s - m_Z^2)} (C_L K_L + C_R K_R), \quad (10)$$

$$T_{ZZ} = \frac{g_Z^4 (a_{ij}^{\tilde{f}})^2}{32(s - m_Z^2)^2} (C_L^2 + C_R^2), \quad (11)$$

and $\kappa(x, y, z) = \sqrt{(x - y - z)^2 - 4yz}$.

Here we use $K_{L,R}$ and $C_{L,R}$ as the left- and right-handed couplings of the electron to the photon and Z boson, respectively,

$$K_L = K_R = 1, \quad C_L = -\frac{1}{2} + s_W^2, \quad C_R = s_W^2. \quad (12)$$

The matrix elements $a_{ij}^{\tilde{f}}$ come from the coupling of $Z\tilde{f}_i\tilde{f}_j$,

$$a_{ij}^{\tilde{f}} = \begin{pmatrix} 4(I_f^{3L} \cos^2 \theta_{\tilde{f}} - s_W^2 e_f) & -2I_f^{3L} \sin 2\theta_{\tilde{f}} \\ -2I_f^{3L} \sin 2\theta_{\tilde{f}} & 4(I_f^{3L} \cos^2 \theta_{\tilde{f}} - s_W^2 e_f) \end{pmatrix}. \quad (13)$$

3 Radiative corrections

The one-loop (renormalized) cross-section σ^{ren} is expressed as

$$\sigma^{\text{ren}}(e^+e^- \rightarrow \tilde{f}_i\tilde{f}_j) = \sigma^{\text{tree}} + \Delta\sigma^{\text{QCD}} + \Delta\sigma^{\text{EW}}, \quad (14)$$

where the symbol Δ denotes UV-finite quantities.

As mentioned in the Introduction, the SUSY-QCD corrections ($\Delta\sigma^{\text{QCD}}$) has already been calculated. In this paper, we give the result for the complete one-loop electroweak corrections ($\Delta\sigma^{\text{EW}}$) using the SUSY invariant dimensional reduction ($\overline{\text{DR}}$) as the regularization scheme. The calculation was performed in the 't Hooft-Feynman gauge, $\xi = 1$.

The electroweak corrections can be split further into the following UV-finite parts as:

$$\Delta\sigma^{\text{EW}} = \Delta\sigma^{\text{Ve}} + \Delta\sigma^{\text{V}\tilde{f}} + \Delta\sigma^{\text{prop}} + \Delta\sigma^{\text{box}}, \quad (15)$$

where $\Delta\sigma^{\text{Ve}}$ and $\Delta\sigma^{\text{V}\tilde{f}}$ stand for the renormalized electron and sfermion vertex, $\Delta\sigma^{\text{prop}}$ for renormalized propagators and $\Delta\sigma^{\text{box}}$ for the box contribution.

The renormalized electron vertex has the form

$$\Delta\sigma^{\text{Ve}} = \frac{N_C}{3} \frac{\kappa^3(s, m_{\tilde{f}_i}^2, m_{\tilde{f}_j}^2)}{16\pi s^2} (\Delta T_{\gamma\gamma}^{Ve} + \Delta T_{\gamma Z}^{Ve} + \Delta T_{ZZ}^{Ve}), \quad (16)$$

where

$$\Delta T_{\gamma\gamma}^{Ve} = \frac{e^4 e_f^2 (\delta_{ij})^2}{s^2} (\Delta e_L K_L + \Delta e_R K_R), \quad (17)$$

$$\Delta T_{\gamma Z}^{Ve} = -\frac{g_Z^2 e^2 e_f a_{ij}^{\tilde{f}} \delta_{ij}}{4s(s - m_Z^2)} (\Delta e_L C_L + \Delta e_R C_R + \Delta a_L K_L + \Delta a_R K_R), \quad (18)$$

$$\Delta T_{ZZ}^{Ve} = \frac{g_Z^4 (a_{ij}^{\tilde{f}})^2}{16(s - m_Z^2)^2} (\Delta a_L C_L + \Delta a_R C_R). \quad (19)$$

$\Delta e_{L,R}$ and $\Delta a_{L,R}$ consist of 3 parts,

$$\Delta e_{L,R} = \delta e_{L,R}^{(v)} + \delta e_{L,R}^{(w)} + \delta e_{L,R}^{(c)}, \quad (20)$$

$$\Delta a_{L,R} = \delta a_{L,R}^{(v)} + \delta a_{L,R}^{(w)} + \delta a_{L,R}^{(c)}. \quad (21)$$

$\delta e_{L,R}^{(v)}$, $\delta a_{L,R}^{(v)}$ correspond to the vertex corrections in Fig. 1, $\delta e_{L,R}^{(w)}$, $\delta a_{L,R}^{(w)}$ are the wave-function corrections and $\delta e_{L,R}^{(c)}$, $\delta a_{L,R}^{(c)}$ correspond to the counterterms.

The renormalized sfermion vertex has a similar form,

$$\Delta\sigma^{V\tilde{f}} = \frac{N_C}{3} \frac{\kappa^3(s, m_{\tilde{f}_i}^2, m_{\tilde{f}_j}^2)}{16\pi s^2} \left(\Delta T_{\gamma\gamma}^{V\tilde{f}} + \Delta T_{\gamma Z}^{V\tilde{f}} + \Delta T_{ZZ}^{V\tilde{f}} \right), \quad (22)$$

where

$$\Delta T_{\gamma\gamma}^{V\tilde{f}} = \frac{e^4 e_f (\Delta e_f)_{ij}}{s^2} (K_L^2 + K_R^2), \quad (23)$$

$$\Delta T_{\gamma Z}^{V\tilde{f}} = -\frac{g_Z^2 e^2}{4s(s - m_Z^2)} (K_L C_L + K_R C_R) ((\Delta e_f)_{ij} a_{ij}^{\tilde{f}} + \delta_{ij} (\Delta a_f)_{ij}), \quad (24)$$

$$\Delta T_{ZZ}^{V\tilde{f}} = \frac{g_Z^4 a_{ij}^{\tilde{f}} (\Delta a_f)_{ij}}{16(s - m_Z^2)^2} (C_L^2 + C_R^2). \quad (25)$$

$(\Delta e_f)_{ij}$ and $(\Delta a_f)_{ij}$ can also be split into vertex corrections, wave-function corrections and counterterms,

$$(\Delta e_f)_{ij} = (\delta e_f)_{ij}^{(v)} + (\delta e_f)_{ij}^{(w)} + (\delta e_f)_{ij}^{(c)}, \quad (26)$$

$$(\Delta a_f)_{ij} = (\delta a_f)_{ij}^{(v)} + (\delta a_f)_{ij}^{(w)} + (\delta a_f)_{ij}^{(c)}. \quad (27)$$

Explicit formulae for the remaining contributions $\Delta\sigma^{\text{prop}}$ and $\Delta\sigma^{\text{box}}$ will be given elsewhere.

Since there are diagrams with photon exchange, we also have to consider the real photon emission (Fig. 3) to cancel the IR–divergencies. The full corrected cross-section is then given by

$$\sigma^{\text{corr}}(e^+e^- \rightarrow \tilde{f}_i \tilde{f}_j) = \sigma^{\text{ren}}(e^+e^- \rightarrow \tilde{f}_i \tilde{f}_j) + \sigma(e^+e^- \rightarrow \tilde{f}_i \tilde{f}_j \gamma). \quad (28)$$

3.1 Vertex and wave-function corrections

The vertex corrections $(\delta e_f)_{ij}^{(v)}$ and $(\delta a_f)_{ij}^{(v)}$ (or $\delta e_{L,R}^{(v)}$ and $\delta a_{L,R}^{(v)}$) originate from the diagrams 1-9 (or 10-15) in Fig. 1 with γ , Z -exchange. The analytic formulae for all the vertex corrections will be given elsewhere.

All wave-function corrections are due to a shift from unrenormalized (bare) fields to the renormalized (physical) ones.

$$\begin{aligned} \tilde{f}_i^0 &= (\delta_{ij} + \frac{1}{2}\delta Z_{ij}) \tilde{f}_j, & \begin{pmatrix} f_L^0 \\ f_R^0 \end{pmatrix} &= \begin{pmatrix} 1 + \frac{1}{2}\delta Z_L & 0 \\ 0 & 1 + \frac{1}{2}\delta Z_R \end{pmatrix} \begin{pmatrix} f_L \\ f_R \end{pmatrix}, \\ \begin{pmatrix} A_\mu^0 \\ Z_\mu^0 \end{pmatrix} &= \begin{pmatrix} 1 + \frac{1}{2}\delta Z_{\gamma\gamma} & \frac{1}{2}\delta Z_{\gamma Z} \\ \frac{1}{2}\delta Z_{Z\gamma} & 1 + \frac{1}{2}\delta Z_{ZZ} \end{pmatrix} \begin{pmatrix} A_\mu \\ Z_\mu \end{pmatrix}. \end{aligned} \quad (29)$$

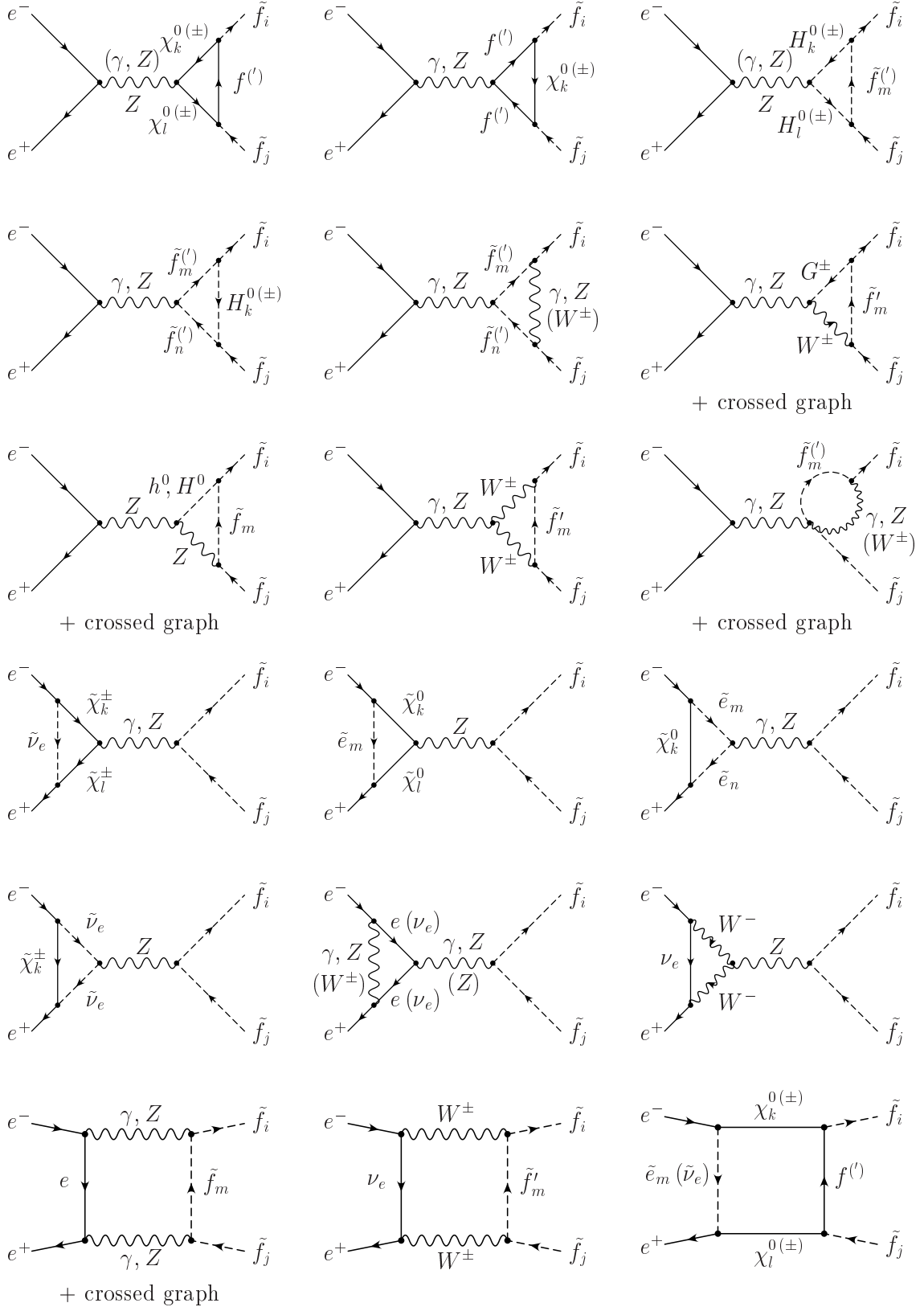


Figure 1: Vertex and box diagrams relevant to the calculation of the electroweak corrections to $e^+e^- \rightarrow \tilde{f}_i \tilde{f}_j$.

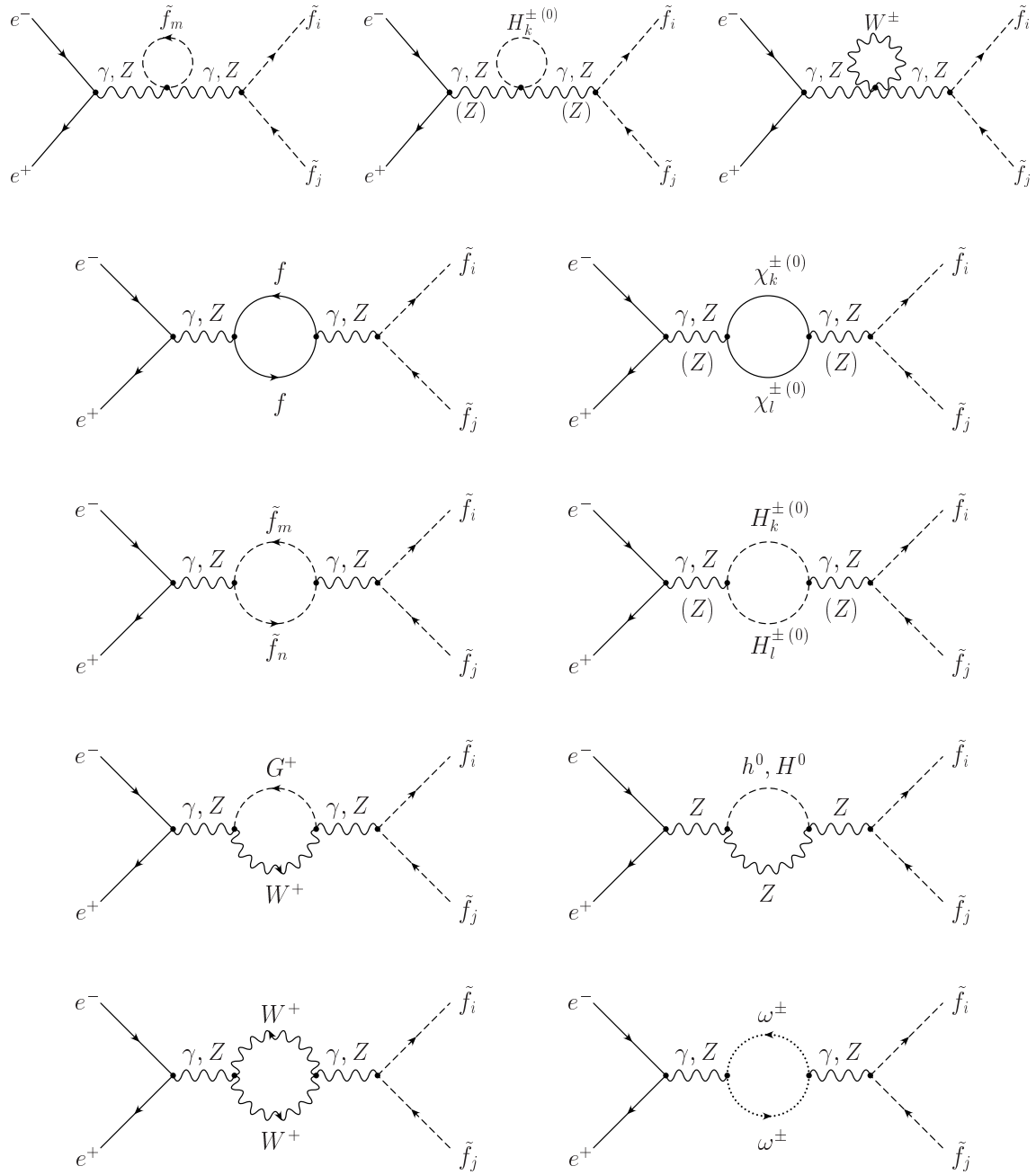


Figure 2: Propagators relevant to the calculation of the electroweak corrections to $e^+e^- \rightarrow \tilde{f}_i\tilde{f}_j$.

The form of the corrections for the left vertex is

$$\delta e_{L,R}^{(w)} = (\delta Z_{L,R} + \frac{1}{2}\delta Z_{\gamma\gamma})K_{L,R} - \frac{1}{2}\frac{g_Z}{e}\delta Z_{Z\gamma}C_{L,R}, \quad (30)$$

$$\delta a_{L,R}^{(w)} = (\delta Z_{L,R} + \frac{1}{2}\delta Z_{ZZ})C_{L,R} - \frac{1}{2}\frac{e}{g_Z}\delta Z_{\gamma Z}K_{L,R}. \quad (31)$$

The wave-function corrections for the right vertex are

$$(\delta e_f)_{ij}^{(w)} = \frac{1}{2}e_f(\delta Z_{ij} + \delta Z_{ji}) + \frac{1}{2}e_f\delta Z_{\gamma\gamma}\delta_{ij} + \frac{1}{8s_Wc_W}a_{ij}^{\tilde{f}}\delta Z_{Z\gamma}, \quad (32)$$

$$(\delta a_f)_{ij}^{(w)} = \frac{1}{2}\sum_{k=1}^2\left(\delta Z_{ki}a_{kj}^{\tilde{f}} + \delta Z_{kj}a_{ik}^{\tilde{f}}\right) + 2s_Wc_We_f\delta_{ij}\delta Z_{\gamma Z} + \frac{1}{2}a_{ij}^{\tilde{f}}\delta Z_{ZZ}. \quad (33)$$

The wave-function renormalization constants are determined by imposing the on-shell renormalization conditions [5, 19]

$$\delta Z_{ii} = -\Re\dot{\Pi}_{ii}^{\tilde{f}}(m_{\tilde{f}_i}^2), \quad \delta Z_{ij} = \frac{2\Re\Pi_{ij}^{\tilde{f}}(m_{\tilde{f}_j}^2)}{m_{\tilde{f}_i}^2 - m_{\tilde{f}_j}^2}, \quad \delta Z_{\gamma\gamma} = -\Re\dot{\Pi}_{\gamma\gamma}(0), \quad (34)$$

$$\delta Z_{ZZ} = -\Re\dot{\Pi}_{ZZ}(m_Z^2), \quad \delta Z_{\gamma Z} = -\frac{2\Re\Pi_{\gamma Z}(m_Z^2)}{m_Z^2}, \quad \delta Z_{Z\gamma} = \frac{2\Re\Pi_{Z\gamma}(0)}{m_Z^2}, \quad (35)$$

$$\begin{aligned} \delta Z_L &= \Re\left[-\Pi_L(m_e^2) - m_e^2(\dot{\Pi}_L(m_e^2) + \dot{\Pi}_R(m_e^2)) + \frac{1}{2m_e}(\Pi_{SL}(m_e^2) - \Pi_{SR}(m_e^2)) \right. \\ &\quad \left. - m_e(\dot{\Pi}_{SL}(m_e^2) + \dot{\Pi}_{SR}(m_e^2))\right], \end{aligned} \quad (36)$$

$$\begin{aligned} \delta Z_R &= \Re\left[-\Pi_R(m_e^2) - m_e^2(\dot{\Pi}_R(m_e^2) + \dot{\Pi}_L(m_e^2)) + \frac{1}{2m_e}(\Pi_{SR}(m_e^2) - \Pi_{SL}(m_e^2)) \right. \\ &\quad \left. - m_e(\dot{\Pi}_{SR}(m_e^2) + \dot{\Pi}_{SL}(m_e^2))\right], \end{aligned} \quad (37)$$

where $\dot{\Pi}(m^2) = \left[\frac{\partial}{\partial k^2}\Pi(k^2)\right]_{k^2=m^2}$ and we use the conventions of [20].

3.2 Counterterms

The counterterms come from the shift from the bare to the physical parameters in the lagrangian. It includes the shifting of $e, m_W, m_Z, \theta_{\tilde{f}}$ defined by

$$e^0 = e + \delta e, \quad m_W^0 = m_W + \delta m_W, \quad m_Z^0 = m_Z + \delta m_Z, \quad \theta_{\tilde{f}}^0 = \theta_{\tilde{f}} + \delta\theta_{\tilde{f}}. \quad (38)$$

The counterterm contributions for both vertices are

$$\delta e_{L,R}^{(c)} = \frac{\delta e}{e}K_{L,R}, \quad (39)$$

$$\delta a_{L,R}^{(c)} = \left[\frac{\delta e}{e} - \left(\frac{\delta m_W}{m_W} - \frac{\delta m_Z}{m_Z}\right) + \frac{1-2s_W}{t_W^2}\left(\frac{\delta m_W}{m_W} - \frac{\delta m_Z}{m_Z}\right)\right]C_{L,R}, \quad (40)$$

$$(\delta e_f)_{ij}^{(c)} = \frac{\delta e}{e}e_f\delta_{ij}, \quad (41)$$

$$(\delta a_f)_{ij}^{(c)} = \left[\frac{\delta e}{e} + \frac{c_W^2 - s_W^2}{s_W^2}\left(\frac{\delta m_W}{m_W} - \frac{\delta m_Z}{m_Z}\right)\right]a_{ij}^{\tilde{f}} + 8e_f c_W^2\left(\frac{\delta m_W}{m_W} - \frac{\delta m_Z}{m_Z}\right)\delta_{ij}, \quad (42)$$

where the contributions containing $\delta\theta_{\tilde{f}}$ were intentionally left out and will be discussed below.

Renormalization of the electric charge e

Since we use as input parameter for α the $\overline{\text{MS}}$ value at the Z -pole, $\alpha \equiv \alpha(m_Z)|_{\overline{\text{MS}}} = e^2/(4\pi)$, we get the counterterm [21, 22]

$$\begin{aligned} \frac{\delta e}{e} = & \frac{1}{(4\pi)^2} \frac{e^2}{6} \left[4 \sum_f N_C^f e_f^2 \left(\Delta + \log \frac{Q^2}{x_f^2} \right) + \sum_{\tilde{f}} \sum_{m=1}^2 N_C^f e_f^2 \left(\Delta + \log \frac{Q^2}{m_{\tilde{f}_m}^2} \right) \right. \\ & \left. - 4 \sum_{k=1}^2 \left(\Delta + \log \frac{Q^2}{m_{\tilde{\chi}_k^+}^2} \right) - \sum_{k=1}^2 \left(\Delta + \log \frac{Q^2}{m_{H_k^+}^2} \right) - 2 \left(\Delta + \log \frac{Q^2}{m_W^2} \right) \right]. \end{aligned} \quad (43)$$

with $x_f = m_Z \forall m_f < m_Z$ and $x_t = m_t$. N_C^f is the colour factor, $N_C^f = 1, 3$ for (s)leptons and (s)quarks, respectively. Δ denotes the UV divergence factor, $\Delta = 2/\epsilon - \gamma + \log 4\pi$.

Renormalization of m_W and m_Z

The masses of the Z -boson and the W -boson are fixed as the physical (pole) masses i.e.

$$\delta m_Z^2 = \Re \Pi_{ZZ}(m_Z^2), \quad \delta m_W^2 = \Re \Pi_{WW}(m_W^2), \quad (44)$$

where

$$\frac{\delta m_Z}{m_Z} = \frac{1}{2} \frac{\delta m_Z^2}{m_Z^2}, \quad \frac{\delta m_W}{m_W} = \frac{1}{2} \frac{\delta m_W^2}{m_W^2}. \quad (45)$$

Renormalization of $\theta_{\tilde{f}}$

The counterterm of the sfermion mixing angle, $\delta\theta_{\tilde{f}}$, is fixed such that it cancels the anti-hermitian part of the sfermion wave-function corrections [6, 23],

$$\delta\theta_{\tilde{f}} = \frac{1}{4} (\delta Z_{12} - \delta Z_{21}) = \frac{1}{2(m_{\tilde{f}_1}^2 - m_{\tilde{f}_2}^2)} \Re \left(\Pi_{12}^{\tilde{f}}(m_{\tilde{f}_2}^2) + \Pi_{21}^{\tilde{f}}(m_{\tilde{f}_1}^2) \right). \quad (46)$$

Including the terms proportional to $\delta\theta_{\tilde{f}}$ in eq. 42 is equivalent to symmetrizing the off-diagonal sfermion wave-function corrections in eq. 34 as [12]

$$\delta Z_{12} = \delta Z_{21} = \frac{\Re \Pi_{12}^{\tilde{f}}(m_{\tilde{f}_2}^2) - \Re \Pi_{21}^{\tilde{f}}(m_{\tilde{f}_1}^2)}{m_{\tilde{f}_1}^2 - m_{\tilde{f}_2}^2}. \quad (47)$$

3.3 Real corrections

The cross-section $\sigma(e^+e^- \rightarrow \tilde{f}_i \tilde{f}_j)$ is IR-divergent owing to the photon mass being zero. This is remedied by introducing a small mass λ and including also the Bremsstrahlung

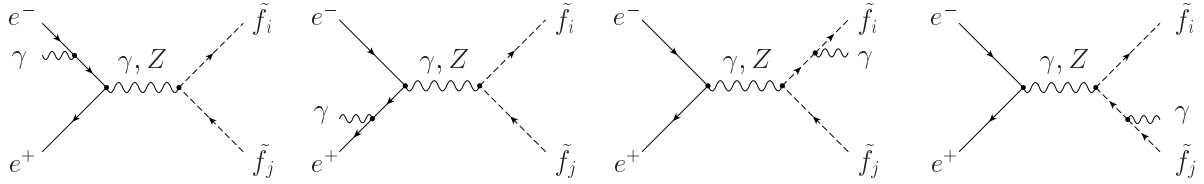


Figure 3: Bremsstrahlung diagrams relevant to the calculation of the real corrections to $e^+e^- \rightarrow \tilde{f}_i \tilde{f}_j \gamma$.

i.e. $\sigma(e^+e^- \rightarrow \tilde{f}_i \tilde{f}_j \gamma)$ as in eq. 28. Summing those two contributions yields an IR-finite result for the physical value $\lambda = 0$.

In our calculation, we used a soft-photon approximation [14] which reproduces the divergence pattern correctly but introduces a cut ΔE on the energy of the radiated photon. The explicit formulae will be given elsewhere.

4 Outline of the calculation

The results presented in this paper come from a full analytic calculation where we have neglected the electron mass ($m_e = 0$) except for the QED corrections.

In the case of this particular process, we can separate off the QED corrections on the basis of Feynman diagrams in a gauge invariant way. The QED corrections consist of all the diagrams that have an additional photon added to the tree-level and therefore also include the whole real corrections. The weak corrections are then UV and IR finite and ΔE independent. All numerical results show only the weak corrections as the QED part is very sensitive to ΔE .

The numerical calculation was performed using the packages LoopTools and FF [15]. The results were checked against the results for the Yukawa approximation presented in [6] where our results match except for a minus sign already pointed out in [7].

Furthermore, we did our own independent calculation based on FeynArts and FormCalc packages [16] checking all individual Feynman diagrams at the amplitude level. In addition, we used the packages to check the complete results using the same renormalization scheme as in the analytical calculation.

We also compared our results with [7] where we were able to reproduce all the results apart from minor differences due to the different renormalization of the fine structure constant.

5 Numerical analysis

In the following numerical examples, we assume $M_{\tilde{Q}} \equiv M_{\tilde{Q}_3} = \frac{10}{9} M_{\tilde{U}_3} = \frac{10}{11} M_{\tilde{D}_3} = M_{\tilde{L}_3} = M_{\tilde{E}_3} = M_{\tilde{Q}_{1,2}} = M_{\tilde{U}_{1,2}} = M_{\tilde{D}_{1,2}} = M_{\tilde{L}_{1,2}} = M_{\tilde{E}_{1,2}}$ for the first, second and third generation soft SUSY breaking masses, and all trilinear couplings are set to a common value A . For the standard model parameters we take $m_Z = 91.1875$ GeV, $m_W = 80.45$ GeV, $\sin^2 \theta_W = 1 - m_W^2/m_Z^2$, $\alpha = 1/127.934$, $m_t = 174.3$ GeV, and $m_b = 4.7$ GeV. M' is fixed

by the gaugino unification relation $M' = \frac{5}{3} \tan^2 \theta_w M$, and the gluino mass is related to M by $m_{\tilde{g}} = (\alpha_s(m_{\tilde{g}})/\alpha) \sin^2 \theta_w M$.

Below we show plots for three different scenarios. On the left, there are the total and tree-level cross-sections for all channels $e^+e^- \rightarrow f_i \tilde{f}_j$, $f = t, b, \tau$, $i = 1, 2$, and on the right we picked out one of the channels and show a separation into the convergent subclasses described in the text above.

One can see that the total corrections in squark production are dominated by SUSY-QCD where the biggest contribution comes from the gluon. The gluino part is small compared to the gluon one as already shown in [5]. At higher energy (1 TeV – 1.5 TeV), other corrections can grow to a size comparable to the SUSY-QCD contribution. The leading EW contribution at high energy comes from the box diagrams. As can be seen in Fig. 4-6, the box diagrams give a negative contribution rising with energy. This can be checked against the Sudakov approximation at high energies [24, 25], where the box contributions give the leading correction. The other two corrections, the vertex and the propagator corrections, are small (below 5%) and almost constant with energy.

The weak corrections computed here have a significant effect in the high energy region, and in the case of squarks act against the SUSY-QCD corrections. In the case of staus they amount to a correction of about -10%.

In addition, we also show the tau-sneutrino production. For detection, it is necessary that not only the decay channel to χ_1^0 is open. Our three scenarios allow decays into charginos. Sneutrino production is the only case where not only the SUSY-QCD corrections are not present but also the Yukawa corrections are small. This is due to the fact that the diagrams including a neutralino or a neutral Higgs boson in the loop are missing. Therefore, the sneutrino production shows a particular dominance of the box corrections. In Fig. 7 one sees that the tree-level is almost identical in two of our scenarios due to the small difference in the sneutrino mass. The total cross-section in the two scenarios is also very similar as the different vertex corrections and the propagator corrections are together below 5% and the boxes give the leading contribution.

6 Conclusion

We have calculated the complete one-loop corrections to stop, sbottom, stau and tau-sneutrino production. The calculation was performed in an analytical way with an independent check using the FeynArts and FormCalc computer packages [16]. Our way of fixing the fine structure constant α gives a higher tree-level cross-section and therefore smaller radiative corrections compared to [7]. The corrections are typically of 5-10% and thus not negligible at a future linear collider.

Acknowledgements

The authors thank A. Arhrib for communication. The authors acknowledge support from EU under the HPRN-CT-2000-00149 network programme and the “Fonds zur Förderung der wissenschaftlichen Forschung” of Austria, project No. P13139-PHY.

SCENARIO 1- gaugino:

The parameters are set to

$$\{M, \mu, A, \tan \beta, m_A, M_{\tilde{Q}}\} = \{200 \text{ GeV}, 1000 \text{ GeV}, -500 \text{ GeV}, 20, 300 \text{ GeV}, 400 \text{ GeV}\}$$

The masses of the sfermions in this scenario are

$$m_{\tilde{t}_{1,2}} = \{276, 520\} \text{ GeV} \quad m_{\tilde{b}_{1,2}} = \{285, 526\} \text{ GeV} \quad m_{\tilde{\tau}_{1,2}} = \{354, 446\} \text{ GeV}$$

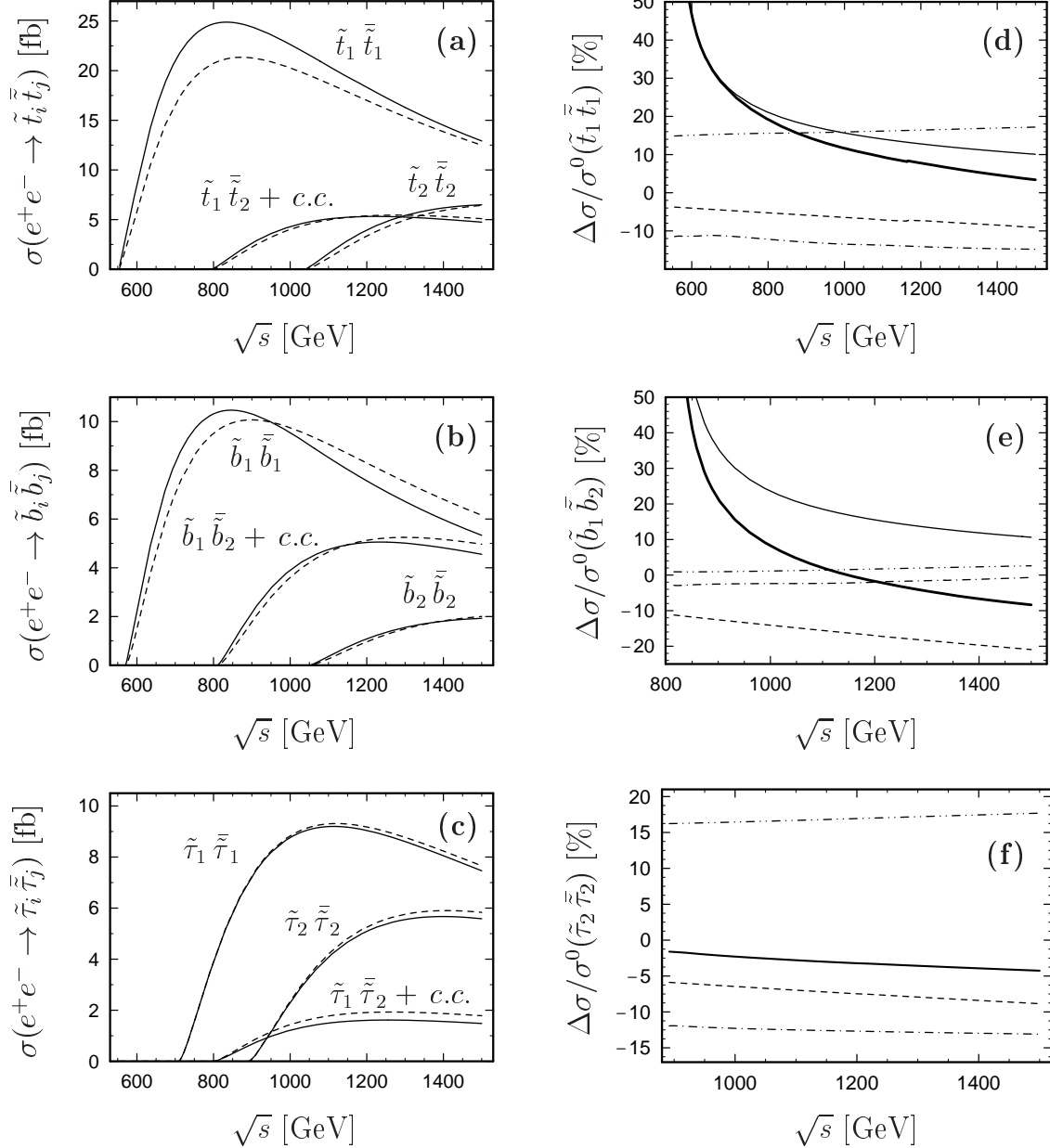


Figure 4: Scenario 1: **(a,b,c)** Total (solid) and tree-level (dashed) cross-sections as a function of \sqrt{s} ; **(d,e,f)** Relative corrections to one of the channels from plots **(a,b,c)** split into convergent subclasses. (thick solid- $\Delta\sigma^{\text{total}}$, solid- $\Delta\sigma^{\text{QCD}}$, dashed- $\Delta\sigma^{\text{box}}$, dash-dotted- $\Delta\sigma^{\text{vertex}}$, dash-dot-dotted- $\Delta\sigma^{\text{prop}}$)

SCENARIO 2- higgsino:

The parameters are set to

$$\{M, \mu, A, \tan \beta, m_A, M_{\tilde{Q}}\} = \{800 \text{ GeV}, -200 \text{ GeV}, 250 \text{ GeV}, 30, 300 \text{ GeV}, 250 \text{ GeV}\}$$

The masses of the sfermions in this scenario are

$$m_{\tilde{t}_{1,2}} = \{200, 360\} \text{ GeV} \quad m_{\tilde{b}_{1,2}} = \{203, 318\} \text{ GeV} \quad m_{\tilde{\tau}_{1,2}} = \{231, 275\} \text{ GeV}$$

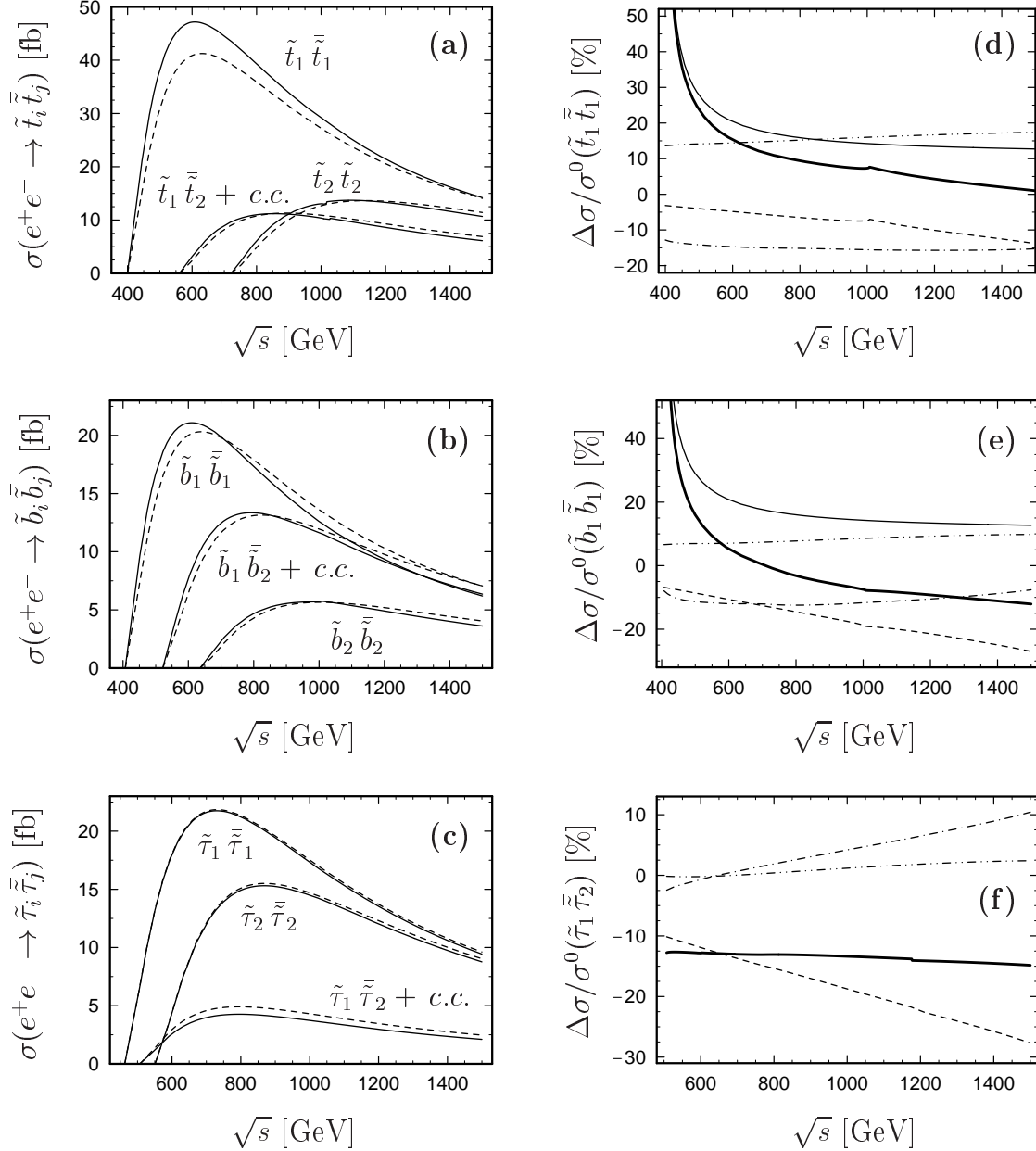


Figure 5: Scenario 2: **(a,b,c)** Total (solid) and tree-level (dashed) cross-sections as a function of \sqrt{s} ; **(d,e,f)** Relative corrections to one of the channels from plots **(a,b,c)** split into convergent subclasses. (thick solid- $\Delta\sigma^{\text{total}}$, solid- $\Delta\sigma^{\text{QCD}}$, dashed- $\Delta\sigma^{\text{box}}$, dash-dotted- $\Delta\sigma^{\text{vertex}}$, dash-dot-dotted- $\Delta\sigma^{\text{prop}}$)

SCENARIO 3- mixed:

The parameters are set to

$$\{M, \mu, A, \tan \beta, m_A, M_{\tilde{Q}}\} = \{200 \text{ GeV}, 200 \text{ GeV}, -800 \text{ GeV}, 10, 300 \text{ GeV}, 400 \text{ GeV}\}$$

The masses of the sfermions in this scenario are

$$m_{\tilde{t}_{1,2}} = \{172, 563\} \text{ GeV} \quad m_{\tilde{b}_{1,2}} = \{398, 446\} \text{ GeV} \quad m_{\tilde{\tau}_{1,2}} = \{396, 409\} \text{ GeV}$$

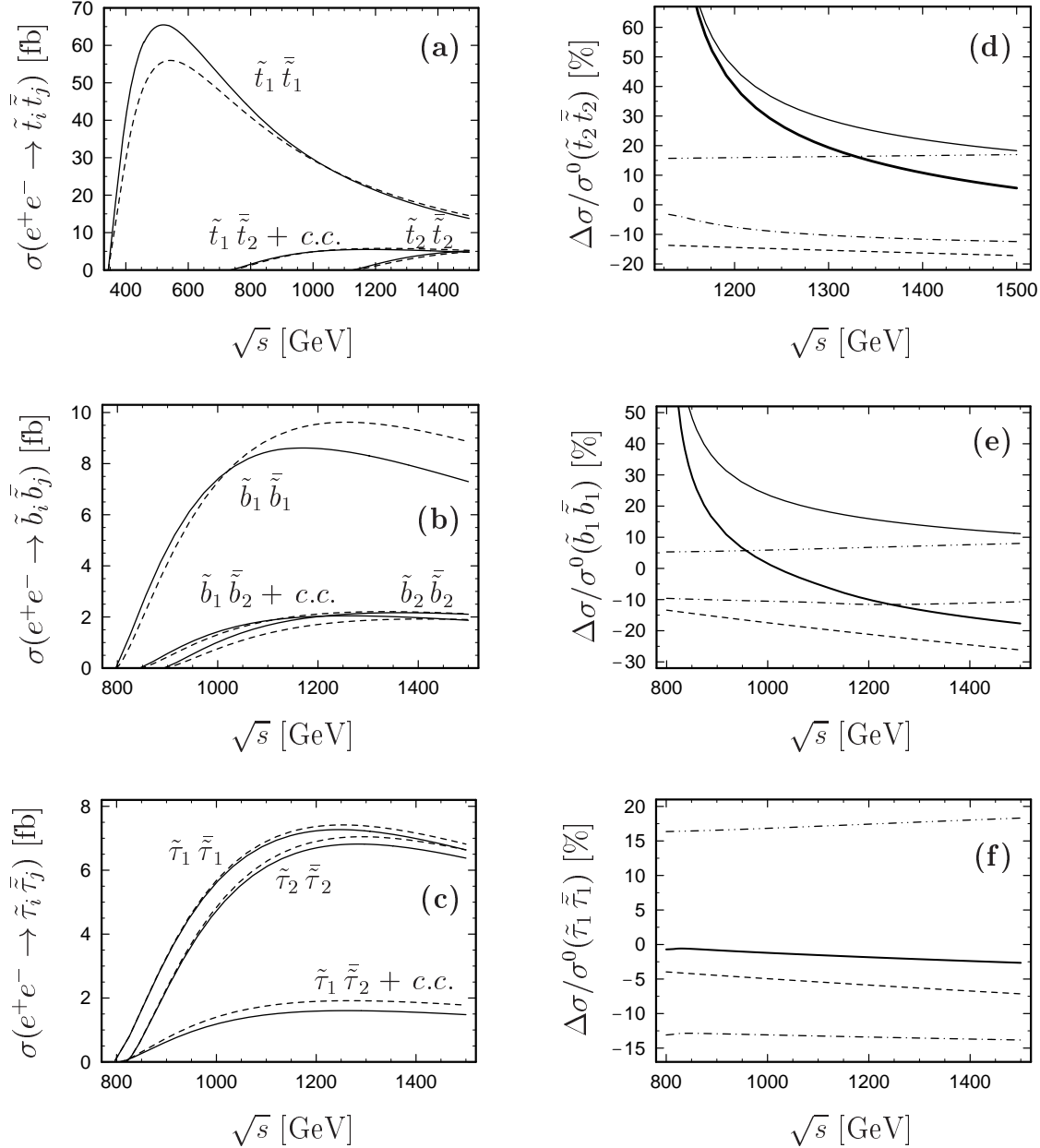


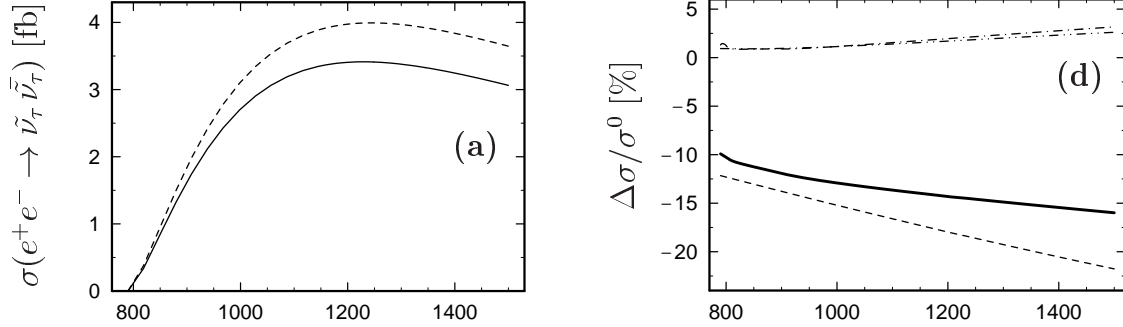
Figure 6: Scenario 3: **(a,b,c)** Total (solid) and tree-level (dashed) cross-sections as a function of \sqrt{s} ; **(d,e,f)** Relative corrections to one of the channels from plots **(a,b,c)** split into convergent subclasses. (thick solid- $\Delta\sigma^{\text{total}}$, solid- $\Delta\sigma^{\text{QCD}}$, dashed- $\Delta\sigma^{\text{box}}$, dash-dotted- $\Delta\sigma^{\text{vertex}}$, dash-dot-dotted- $\Delta\sigma^{\text{prop}}$)

SNEUTRINO PLOTS:

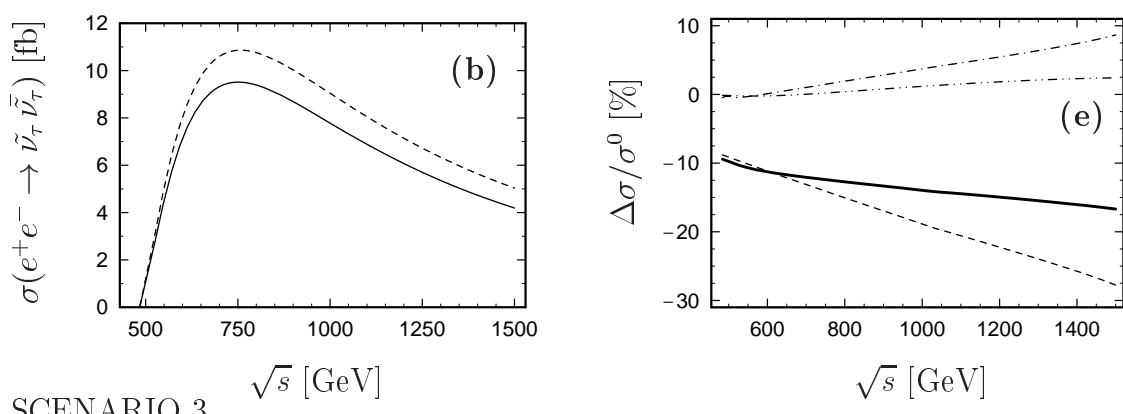
Here we show the sneutrino production in all three scenarios. The masses of the sneutrino in the scenarios are

$$m_{\tilde{\nu}_\tau} = 394.795 \text{ GeV} \quad m_{\tilde{\nu}_\tau} = 242 \text{ GeV} \quad m_{\tilde{\nu}_\tau} = 394.873 \text{ GeV}$$

SCENARIO 1



SCENARIO 2



SCENARIO 3

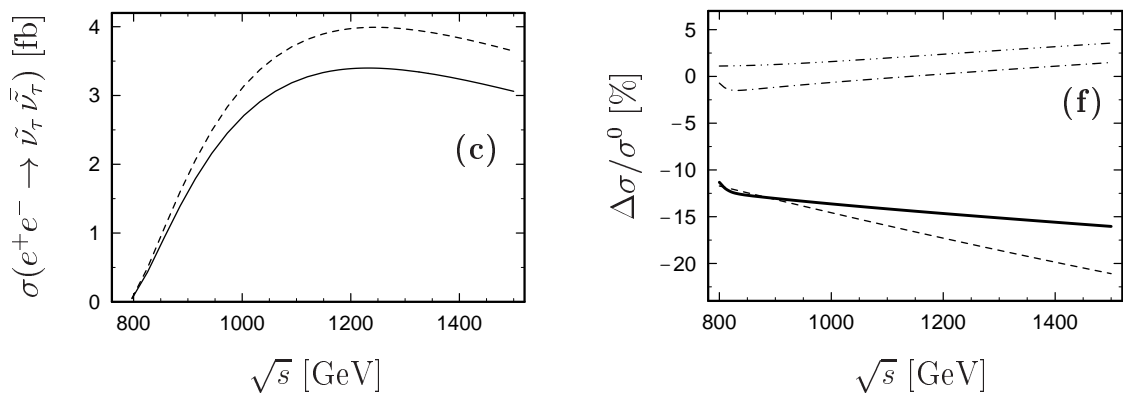


Figure 7: Sneutrino plots: (a,b,c) Total (solid) and tree-level (dashed) cross-sections as a function of \sqrt{s} ; (d,e,f) Relative corrections split into convergent subclasses. (thick solid- $\Delta\sigma^{\text{total}}$, dashed- $\Delta\sigma^{\text{box}}$, dash-dotted- $\Delta\sigma^{\text{vertex}}$, dash-dot-dotted- $\Delta\sigma^{\text{prop}}$)

References

- [1] TESLA Technical Design Report, DESY 2001-011;
ECFA/DESY LC Physics Working Group, [arXiv:hep-ph/0106315];
ACFA Linear Collider Working Group, [arXiv:hep-ph/0109166];
Proceedings of the *APS/DPF/DPB Summer Study on the Future of Particle Physics (Snowmass 2001)*, ed. N. Graf [arXiv:hep-ex/0106056].
- [2] M. Drees, K. Hikasa, Phys.Lett. **B252** (1990) 127;
K. Hikasa, J. Hisano, Phys.Rev. **D54** (1996) 1908 [arXiv:hep-ph/9603203].
- [3] W. Beenakker, R. Höpker, P. M. Zerwas, Phys. Lett. **B349** (1995) 463 [arXiv:hep-ph/9501292].
- [4] A. Arhrib, M. Capdequi-Peyranere, A. Djouadi, Phys. Rev. **D52** (1995) 1404 [arXiv:hep-ph/9412382].
- [5] H. Eberl, A. Bartl, W. Majerotto, Nucl. Phys. **B472** (1996) 481 [arXiv:hep-ph/9603206].
- [6] H. Eberl, S. Kraml, W. Majerotto, JHEP **9905** (1999) 016 [arXiv:hep-ph/9903413].
- [7] A. Arhrib, W. Hollik, [arXiv:hep-ph/0311149] to appear in Eur.Phys.J.C.
- [8] A. Freitas, D. J. Miller, P. M. Zerwas, Eur.Phys.J. **C21** (2001) 361-368 [arXiv:hep-ph/0106198];
A. Freitas, A. von Manteuffel, P. M. Zerwas, [arXiv:hep-ph/0310182].
- [9] T. Fritzsch, W. Hollik, Eur.Phys.J. **C24** (2002) 619-629 [arXiv:hep-ph/0203159].
- [10] W. Hollik, H. Rzehak, [arXiv:hep-ph/0305328], to appear in Eur.Phys.J.
- [11] A. Bartl *et al.*, Phys. Lett. **B402** (1997) 303-313 [arXiv:hep-ph/9701398]
- [12] H. Eberl, M. Kincel, W. Majerotto and Y. Yamada, Phys. Rev. **D64** (2001) 115013 [arXiv:hep-ph/0104109].
- [13] W. Majerotto, [arXiv:hep-ph/0209137], in Proceedings of the *10th International Conference on Supersymmetry and Unification of Fundamental Interactions (SUSY02)*, ed. P. Nath, P. M. Zerwas, Hamburg 2002.
- [14] A. Denner, Fortschr. Phys. **41** (1993) 307.
- [15] G. J. Oldenborgh, Comput. Phys. Commun. **66** (1991) 1;
T. Hahn, Acta Phys. Polon. **B30** (1999) 3469.
- [16] J. Küblbeck, M. Böhm, A. Denner, Comput. Phys. Commun. **60** (1990) 165;
T. Hahn, Comput. Phys. Commun. **140** (2001) 418;
T. Hahn, C. Schappacher, Comput. Phys. Commun. **143** (2002) 54;
T. Hahn, M. Perez-Victoria, Comput. Phys. Commun. **118** (1999) 153.

- [17] J. F. Gunion, H. E. Haber, G. L. Kane and S. Dawson, *The Higgs Hunter's Guide*, Addison-Wesley (1990).
- [18] J. F. Gunion, H. E. Haber, *Nucl. Phys.* **B272** (1986) 1; **B402** (1993) 567 (E).
- [19] M. Böhm, W. Hollik and H. Spiesberger, *Fortschr. Phys.* **34** (1986) 687.
- [20] C. Weber, H. Eberl, W. Majerotto, *Phys. Rev.* **D68** (2003) 0930011 [[arXiv:hep-ph/0308146](#)].
- [21] C. Weber, H. Eberl, W. Majerotto, *Phys. Lett.* **B572** (2003) 56 [[arXiv:hep-ph/0305250](#)].
- [22] H. Eberl, M. Kincel, W. Majerotto and Y. Yamada, *Nucl. Phys.* **B625** (2002) 372 [[arXiv:hep-ph/0111303](#)].
- [23] J. Guasch and J. Sola, W. Hollik, *Phys. Lett.* **B437** (1998) 88 [[arXiv:hep-ph/9802329](#)].
- [24] M. Beccaria, M. Melles, F. M. Renard, C. Verzegnassi, *Phys. Rev.* **D65** (2002) 093007 [[arXiv:hep-ph/0112273](#)].
- [25] M. Beccaria, M. Melles, F. M. Renard, S. Trimarchi, C. Verzegnassi, *Int. J. Mod. Phys.* **A18** (2003) 5069-5098 [[arXiv:hep-ph/0304110](#)].